35th Annual International Conference of the IEEE EMBS
Osaka, Japan, 3 - 7 July, 2013

Preamplifiers for non-contact capacitive biopotential measurements*

GuoChen Peng[1], Zeljko Ignjatovic[1], and Mark F. Bocko[1]

Abstract— **Non-contact biopotential sensing is an attractive measurement strategy for a number of health monitoring applications, primarily the ECG and the EEG. In all such applications a key technical challenge is the design of a low-noise trans-impedance preamplifier for the typically low-capacitance, high source impedance sensing electrodes. In this paper, we compare voltage and charge amplifier designs in terms of their common mode rejection ratio, noise performance, and frequency response. Both amplifier types employ the same operational-transconductance amplifier (OTA), which was fabricated in a 0.35um CMOS process. The results show that a charge amplifier configuration has advantages for small electrode-to-subject coupling capacitance values (less than 10 pF - typical of noncontact electrodes) and that the voltage amplifier configuration has advantages for electrode capacitances above 10 pF.**

I. INTRODUCTION

The ability to make low noise biopotential measurements provides the foundation for a number of important medical sensing applications, primarily the electrocardiogram (ECG), the electroencephalogram (EEG), and the electromyogram (EMG). The electrode types used in such sensing applications fall into the following categories: wet conductive gel electrodes, dry contact electrodes, insulated electrodes, and non-contact, stand-off electrodes [1]. The overall source impedance of wet-gel, dry-contact, and insulated electrodes typically is much smaller than the source impedance of stand-off non-contact electrodes, often by a factor of 1000 or more. For low source impedance (a high coupling capacitance in combination with low series resistance), a voltage follower amplifier typically is employed. To minimize the gain error of the amplifier it is useful to keep the source capacitance much larger than the preamp input capacitance, which includes unknown and difficult to control stray capacitances. For non-contact electrodes, the source capacitance may be less than 1pF so very strict control of the stray capacitance at the preamp input is required to minimize gain uncertainty. A trans-impedance charge amplifier [2] is an alternative option to consider for low capacitance source electrodes. In this paper we explore biopotential measurements employing weakly coupled electrodes (low capacitance) and make a comparison of the relative merits of the standard voltage follower and charge amplifier configurations.

*This work was supported by Blue Highway and the New York State Foundation for Science, Technology and Innovation, and in part by the Eunice Kennedy Shriver National Institute of Child Health Development Grant R01HD060789.

[1]G. Peng, Z. Ignjatovic and M. F. Bocko are with the Electrical and Computer Engineering Department, University of Rochester, Rochester, NY 14627-0231 USA gupeng;ignjatov;bocko at ece.rochester.edu

Traditionally, non-contact sensors have been built with a high input impedance voltage follower amplifier (VA), [1] and [3]. Due to the small source capacitance, the input capacitance of the front-end VA must be kept extremely small or otherwise neutralized, however this can degrade the noise performance [4]. To cope with small bioelectric signals, a charge amplifier (CA) design is a promising option because its gain is independent of the input capacitance of the preamplifier [5]. Furthermore, shielding in the CA configuration is straightforward and the low-frequency cutoff is independent of the source capacitance. However, the challenge of using a CA is that its gain depends on the source capacitance, which may be modulated by the relative motion of the subject and the electrodes.

In this paper, we compare the performance of a voltage and charge amplifier configurations with respect to the requirements for differential biopotential recording systems for different ranges of source capacitance. We begin this in the following section with an analysis and a comparison of the predicted performance of the VA and CA configurations. In section III we present experimental results with an operational transconductance amplifier (OTA), fabricated in a 0.35um CMOS process, which are followed by a brief conclusion.

II. AMPLIFIER ANALYSIS

In this section, we compare the voltage and charge mode amplifier configurations in terms of their common mode rejection ratio (CMRR), frequency response, and noise performance.

A. CMRR

Interference from ac power lines or other common-mode signals will appear at the amplifier output if the CMRR of the sensor system is low [6]. Although such interfering signals can be filtered out in principle this requires additional circuitry and amplifier saturation remains as a possible problem. In clinical ECG applications the driven right leg (DRL) technique is commonly used to achieve high CMRR; this method can be employed with either a VA or CA. However, the DRL method is not feasible for use in an ambulatory setting, which is of interest here. Thus in the following we analyze the CMRR for both the VA and CA amplifier types in a conventional differential mode configuration.

In Fig. 1 a generic differential amplifier is shown. The input stages $H_1(s)$ and $H_2(s)$ may be implemented as either a VA or CA, as indicated in the figure. For the VA the differential output $V_{od,vol}$ and common mode output $V_{ocm,vol}$ can be expressed as,

978-1-4577-0216-7/13/$26.00 ©2013 IEEE

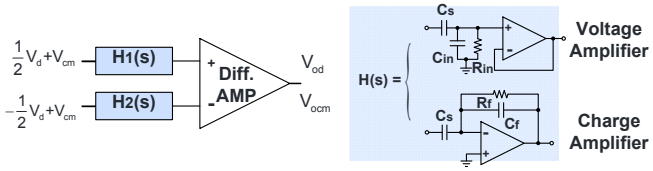

Fig. 1. A generic differential amplifier where the two input channels may be implemented as either a voltage amplifier or a charge amplifier.

$$V_{od,vol} = \frac{1}{2}V_d H_1(s) - \left(-\frac{1}{2}\right) V_d H_2(s)$$
$$= \frac{1}{2}V_d \left[\frac{sR_{in}C_{s1}}{1+sR_{in}(C_{s1}+C_{in})} + \frac{sR_{in}C_{s2}}{1+sR_{in}(C_{s2}+C_{in})}\right]$$
$$= V_d \cdot A_{d\_vol} \quad (1)$$

$$V_{ocm,vol} = V_{cm}H_1(s) - V_{cm}H_2(s)$$
$$= V_{cm} \left[\frac{sR_{in}C_{s1}}{1+sR_{in}(C_{s1}+C_{in})} - \frac{sR_{in}C_{s2}}{1+sR_{in}(C_{s2}+C_{in})}\right]$$
$$= V_{cm} \cdot A_{cm\_vol} \quad (2)$$

where $H_1(s)$ and $H_2(s)$ are the transfer functions of the two voltage amplifiers and C_{s1} and C_{s2} are the source capacitances at each differential input. R_{in} and C_{in} are the amplifier input resistance and capacitance, respectively. To simplify the calculations, we assume that both input channels have equal input resistance and capacitance. Therefore, the CMRR of the VA can be expressed as:

$$CMRR_{vol} = \left|\frac{A_{d\_vol}}{A_{cm\_vol}}\right|$$
$$= \frac{1}{2}\left[\frac{C_{s1}+C_{s2}+sR_{in}\left(2C_{s1}C_{s2}+C_{in}(C_{s1}+C_{s2})\right)}{C_{s1}-C_{s2}+sR_{in}C_{in}(C_{s1}C_{s2})}\right] \quad (3)$$

We define α, the source capacitance mismatch as follows, C_{s1}=C_s(1+α), C_{s2}=C_s(1-α). We estimate that in practical cases the mismatch term α may exceed 50% due to a significant motion of the non-contact electrodes with respect to the test subject. Thus, the CMRR can be written as,

$$CMRR_{vol} = \frac{1}{2\alpha} + \frac{(1-\alpha^2)sR_{in}C_s}{2\alpha(1+sR_{in}C_{in})} \quad (4)$$

Similarly, the CMRR of the differential CA can be derived as follows,

$$V_{od,ch} = \frac{1}{2}V_d H_1(s) - \left(-\frac{1}{2}\right) V_d H_2(s)$$
$$= -\frac{1}{2}V_d \left[\frac{-sR_fC_{s1}}{1+sR_fC_f} + \frac{-sR_fC_{s2}}{1+sR_fC_f}\right]$$
$$= V_d \cdot A_{d\_ch} \quad (5)$$

$$V_{ocm,ch} = V_{cm}H_1(s) - V_{cm}H_2(s)$$
$$= -V_{cm} \left[\frac{-sR_fC_{s1}}{1+sR_fC_f} - \frac{-sR_fC_{s2}}{1+sR_fC_f}\right]$$
$$= V_{cm} \cdot A_{cm\_ch} \quad (6)$$

$$CMRR_{ch} = \left|\frac{A_{d\_ch}}{A_{cm\_ch}}\right| = \frac{1}{2}\left(\frac{C_{s1}+C_{s2}}{C_{s1}-C_{s2}}\right) = \frac{1}{2\alpha} \quad (7)$$

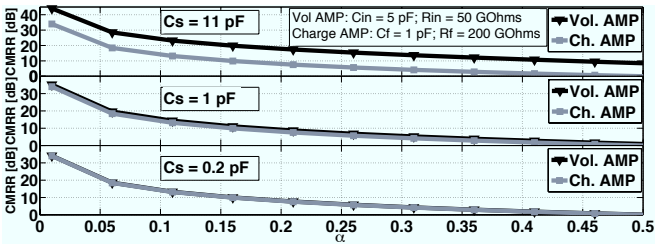

Fig. 2. CMRR vs. mismatch ratio of coupling capacitance α for a voltage amplifier and a charge amplifier. Other components in the circuits are assumed to be perfectly matched. Both CMRRs behave identically when source capacitance becomes small, 0.2pF in the example given here.

We note that the CMRR of the VA (4) has an additional term in comparison to the CMRR of the CA (7). The CMRR advantage of the voltage amplifier comes about from the feature that the input impedance R_{in} of the VA is grounded which enables a degree of control with respect to the resistive charging path for common mode interference. In contrast, since the feedback resistor R_f of the CA is not grounded, the common mode interferences may not be attenuated as much as in the VA. As shown in (4), since the source capacitance C_s and the input capacitance C_{in} are equally small, the way to increase CMRR is to raise R_{in}. In addition, as shown in (4), the CMRR exhibits a high-pass characteristic, where the second term becomes dominant for high frequency common mode signals.

In order to compare (4) and (7), both equations were numerically simulated at mid-band frequency in MATLAB using the typical values given in Fig. 2. The VA displays better CMRR than the CA, when the source capacitance is comparable to the input capacitance. However, when C_s is small in comparison to C_{in} (20% or less) the CMRR of both systems is nearly the same. In a non-contact interface the gap between the electrodes and the test subject are millimeters or greater, and therefore the coupling capacitance typically is small. Overall, the CMRR of the voltage amplifier configuration is superior to that of charge amplifier configuration.

B. Frequency Response

Since the gain of the VA shown in Fig. 1 exhibits a non-linear dependence on the source capacitance C_s, its frequency response may become unstable and difficult to predict for small values of the source capacitance. In contrast, the gain of the CA is determined simply by the ratio of C_s and C_f. Fig. 3 shows the gain simulation for the two amplifier configurations with typical parameters. The gain of the VA approaches to 0 dB for larger source capacitances, above a few pF. Therefore, the CA might have better gain linearity in the weak coupling, small source capacitance regime, which is typical of non-contact applications.

In addition, the high pass corner frequency ω_0 of the VA, $\omega_0 = 1/R_{in}(C_{in}+C_s)$, with the mismatches α in II-A, can influence the accuracy of the subsequent differential measurements. In contrast, the high-pass corner frequency of the CA is independent of the coupling capacitance C_s and

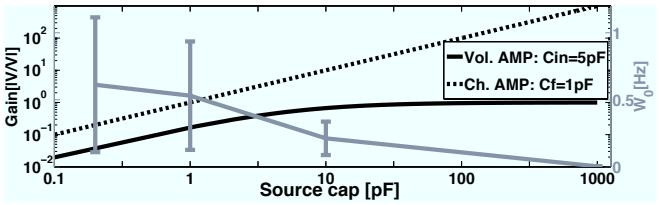

Fig. 3. Mid-band gain simulation of the voltage and charge mode amplifier for different values of coupling source capacitances. The voltage amplifier highpass corner cutoff from C_s = 0.2pF is also shown for $\pm 50\%$ mismatch. The charge amplifier has a constant corner frequency at 0.5Hz, which is not shown.

can be kept constant. Herein, we define the corner frequency of the VA including the mismatch variation term as shown in (8),

$$\omega_{0,mis} = \omega_0 \pm \Delta\omega_0|_{\alpha=50\%} \tag{8}$$

where we consider an extreme case scenario of α equal to 50%. The values of ω_0 are computed versus source capacitance C_s, and are shown in Fig. 3. It can be seen that the corner frequency and its variations due to the mismatch both decrease with higher source capacitance. In general, it is preferred to keep the corner frequency of the VA far below the signal frequencies of interest throughout the entire span of source capacitance values.

C. Noise Performance

The noise of both amplifiers is dependent upon the source capacitance value. We are interested in finding the input referred noise at the source of the electrode-subject interface. First, we model the noise of the operational transconductance amplifier (OTA) with voltage noise source V_n and current noise source I_n at the input transistors of the OTA. Then, we derive an expression for the input referred noise power of both the VA and CA; these expressions are given in (9) and (10), where Δf represents the noise bandwidth.

$$\overline{V_{n,vol}^2} = \overline{V_n^2}(\frac{C_s + C_{in}}{C_s})^2 + \frac{4kT\Delta f}{R_{in}^2(sC_s)^2} + \frac{\overline{I_n^2}}{(sC_s)^2} \tag{9}$$

$$\overline{V_{n,ch}^2} = \overline{V_n^2}(\frac{C_s + C_{in} + C_f}{C_s})^2 + \frac{4kT\Delta f}{R_f(sC_s)^2} + \frac{\overline{I_n^2}}{(sC_s)^2} \tag{10}$$

Normally, R_{in} and R_f are large (several tens of Gigaohms) in comparison to the source impedance, which minimizes its effect. Moreover, the current noise I_n of a CMOS transistor is small (femtoamperes). Therefore, the last two terms in (9) and (10) can be neglected in the input referred noise calculation.

The simulation results and the simplified noise expressions for both amplifiers are shown in Fig. 4 where the input referred noise is the product of the voltage noise V_n and the noise gain. For the given parameters, the noise powers of the VA and CA are approximately equal whenever C_f is much less than the sum of C_s and C_{in}. However, in non-contact scenarios the source capacitance can be less than 1pF, which is comparable to C_f. Therefore, for small source capacitance, the VA exhibits better noise performance than the CA.

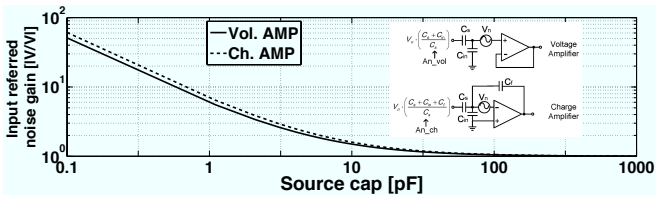

Fig. 4. Input referred noise gain simulation of the voltage amplifier and charge amplifier. The noise gain is almost equal for coupling capacitance values greater than 15pF. The voltage amplifier has better noise performance when the coupling capacitance is small, i.e., below 10pF.

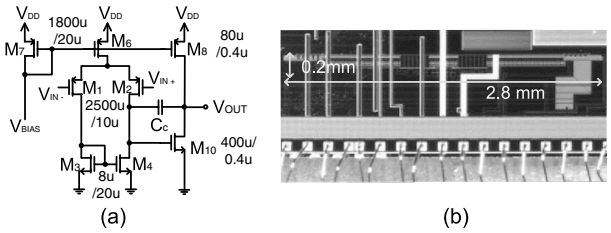

Fig. 5. (a) Two-stage OTA with transistor size indicated. (b) Microphotograph of 2.8 mm x 0.2 mm low noise front-end OTA.

III. EXPERIMENTAL RESULTS

To experimentally verify the comparative performance of the VA and CA discussed above, we employed an identical OTA but different closed loop configurations to implement both types of amplifiers. The OTA design that we employed is a standard two-stage topology amplifier [7] with PMOS input transistors. The chip was fabricated in a 0.35um CMOS process, see Fig. 5. The measured input capacitance of the OTA was about 30pF. This relatively large input capacitance is due to the large input transistors employed in order to minimize the flicker noise component of the OTA.

A. CMRR

To measure CMRR as predicted in Fig. 2, two source capacitance values, 11pF and 2pF, were used for the comparisons, which is typical of weakly coupled stand-off sensor electrodes. The CA feedback resistor and capacitor were selected to be 26.6 GOhms and 12pF, respectively. For each α value, different value capacitors, C_{s1} and C_{s2}, were coupled to the input node of the two OTAs for both the VA and CA configurations. The amplifiers were then coupled to a Stanford Research low noise amplifier (Model SR560) to make differential readings. Five CMRR measurements were recorded for each mismatch α. The results, given in Fig. 6, show that the CMRR's for the VA and CA amplifier configurations are nearly the same for all values of mismatch parameter for small source capacitance (2pF). For the larger source capacitance (11pF) the VA CMRR is higher than that of the CA, as predicted in the simulation. The measured CMRR values were much lower than the values obtained in simulation, which may have arisen from the higher common mode gain because a high value of input capacitance was employed in the OTA and there are small mismatches between the differential components on boards.

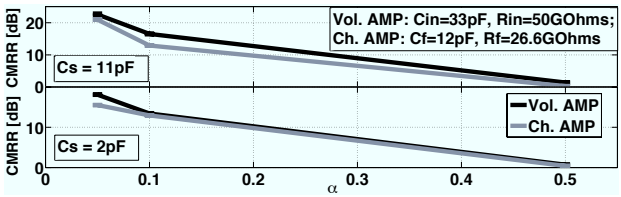

Fig. 6. CMRR measurements for source capacitance values of 11pF and 2pF with mismatch α from 0.05 to 0.5 for both voltage and charge amplifiers. The error bars are provided for each measurement. The result indicates that the smaller coupling capacitance is, the closer the values of CMRR.

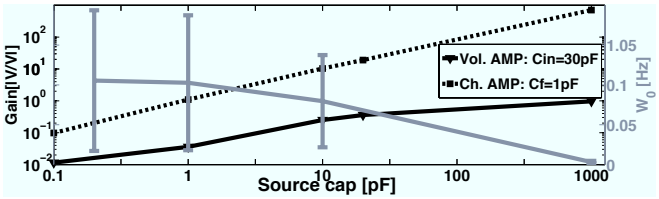

Fig. 7. Mid band gain measurements for source capacitance from 0.1pF to 1nF. For the charge amplifier, the feedback capacitor was 1pF.

B. Frequency Response

The frequency response of the VA and CA amplifier configurations were recorded for several values of source capacitance down to 0.1pF. For the CA, the feedback capacitor was selected to be 1pF to prevent saturation at 1nF source capacitance. The mid-band gains were recorded with a spectrum analyzer to assure that the amplifiers were being operated above the high pass corner frequency. The results in Fig. 7 show the predicted linear relationship between the gain and the source capacitance of the CA. It is worth noting that in the weakly coupled case (0.1pF) the CA still has a precisely known gain (0.1pF/1pF). Finally, the VA corner cutoff was also recorded.

C. Noise Performance

The input referred noise for both amplifier configurations was measured five times using a low noise amplifier with a gain of 500 between a FFT spectrum analyzer and the amplifiers. Measurements were repeated with several source capacitor values. The system response was measured in situ by the spectrum analyzer for each noise measurement. A noise bandwidth of 100Hz was used to be representative of ECG requirements [8] and we did not employ a 60Hz filter to remove the ac line noise. The CA feedback capacitor values used were 2pF, 15pF, and 40pF for the noise comparisons with the VA. The results are shown in Fig. 8. For low noise applications, the value of the feedback capacitor should be small compared to the source and input capacitances. In this case, both amplifiers exhibit the same noise performance. It also is worth pointing out that a small feedback capacitor will give high gain even for small source capacitance values, which makes it unnecessary to include a second gain stage as required in the VA configuration. The experimental results also show that the fabricated OTA has a noise level less than $1\mu Vrms$ over the 100 Hz signal band referred to the input

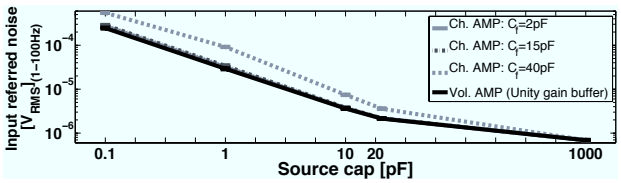

Fig. 8. Noise measurements for source capacitance from 0.1pF to 1nF with error bars. For the charge amplifier, the feedback capacitor value was selected to be 1pF, 15pF, and 40pF.

TABLE I
PREFERRED PREAMPLIFIER FOR HIGH AND LOW SOURCE CAPACITANCES

Parameter	High source cap.	Low source cap.
CMRR	Voltage amp.	Both
Frequency response	Both	Charge amp.
Noise	Both	Both
Overall	*Voltage amp.*	*Charge amp.*

transistor in the high source coupling regime.

IV. CONCLUSIONS

The VA and CA are both viable options for biopotential preamplifiers. In summary, see Table I for a comparison, at higher source capacitor values (greater than 100pF), the VA may be preferred due to its better CMRR, stable gain, and low noise. For lower source capacitance values, the CA is an attractive alternative due to its linear gain response, CMRR value nearly the same as that of the VA, and noise performance for small CA feedback capacitor values that is comparable to that of the VA. Finally, in our implementation of a non-contact ECG sensor [9] we monitor the source capacitance value and then compensate the output for motion induced gain modulation, which is greatly facilitated by the linear response characteristics of the CA configuration.

REFERENCES

[1] Y. Chi, T.-P. Jung, and G. Cauwenberghs, "Dry-contact and noncontact biopotential electrodes: Methodological review," *Biomedical Engineering, IEEE Reviews in*, vol. 3, pp. 106 –119, 2010.

[2] R. Harrison and C. Charles, "A low-power low-noise cmos amplifier for neural recording applications," *Solid-State Circuits, IEEE Journal of*, vol. 38, no. 6, pp. 958 – 965, june 2003.

[3] Y. G. Lim, K. K. Kim, and S. Park, "Ecg measurement on a chair without conductive contact," *Biomedical Engineering, IEEE Transactions on*, vol. 53, no. 5, pp. 956 –959, may 2006.

[4] H. Fein, "Solid-state electrometers with input-capacitance neutralization," *Biomedical Engineering, IEEE Transactions on*, vol. BME-11, no. 1, pp. 13 –18, jan. 1964.

[5] M. Sampietro, L. Fasoli, and G. Bertuccio, "Source follower or charge amplifier? an experimental comparison using a detector with integrated electronics," *Nuclear Science, IEEE Transactions on*, vol. 43, no. 4, pp. 2413 –2418, aug 1996.

[6] J. G. Webster, *Medical instrumentation, application and design*. Wiley, 2010.

[7] B. Razavi, *Design of analog CMOS integrated circuits*. McGraw Hill, 2001.

[8] G. A. Mirvis DM and B. AS., "Instrumentation and practice standards for electrocardiographic monitoring in special care units," *Circulation*, pp. 79–464, 1989.

[9] G. Peng and M. Bocko, "A low noise, non-contact capacitive cardiac sensor," in *Engineering in Medicine and Biology Society (EMBC), 2012 Annual International Conference of the IEEE*, 28 2012-sept. 1 2012, pp. 4994 –4997.